



ISSN 0975-413X
CODEN (USA): PCHHAX

Der Pharma Chemica, 2016, 8(19):175-181
(<http://derpharmachemica.com/archive.html>)

Electrochemical investigation of mineral compound as corrosion inhibitor on brass in artificial tap water (ATW)

M. Nihorimbere¹, Y. Kerroum¹, S. Echihi¹, A. Guenbour¹, A. Bellaouchou¹, M. Kacimi¹,
R. Touri^{2,3} and A. Zarrouk⁴

¹Laboratoire des Matériaux, Nanotechnologies et Environnement, Faculté des Sciences de Rabat, Université Mohammed V-Rabat, Morocco

²Laboratoire d'Ingénierie des Matériaux et d'Environnement : Modélisation et Application, Faculté des Sciences, Université Ibn Tofail, BP 133, Kénitra 14 000, Morocco

³Centre Régional des Métiers de l'Éducation et de la Formation (CRMEF), Avenue Allal Al Fassi, Madinat Al Irfane BP 6210 Rabat, Morocco

⁴LC2AME-URAC 18, Faculty of Science, First Mohammed University, PO Box 717, 60 000 Oujda, Morocco

ABSTRACT

The paper presents the results of corrosion behaviour of brass in artificial tap water (ATW) and the inhibitor effect of mineral compound (MI) using two different electrochemical methods were used, classical potentiodynamic measurement and electrochemical impedance spectroscopy (EIS). The inhibitory effectiveness of corrosion increases with the concentration of inhibitor and reaches 86 % at 40 ppm. Potentiodynamic polarization measurements indicate that MI compound is cathodic type inhibitor. Appropriate electric equivalent circuit model was used to calculate the impedance parameters. The values of the charge transfer resistance, obtained from impedance plots of brass, increased with increasing inhibitor concentration but those of capacity of the double layer decrease, leading to the formation of a protective film.

Keywords: Brass, Corrosion, Mineral inhibitor, Artificial Tap Water (ATW), Electrochemical methods.

INTRODUCTION

Copper and its alloys exhibit high electrical and thermal conductivity, high formability, machinability and strength, hence they are extensively used as a material in heating and cooling systems, potable water pipes, valves, heat exchanger tubes, wire, screens, shafts, roofing, bearings, stills, tanks and printed circuits. Brass has been widely used for shipboard condensers, power plant condensers and petrochemical heat exchangers [1-3]. These materials also have good corrosion resistance to acids as well as chloride-containing media [4-7]. Dezincification of brass is one of the well-known and common processes by means of which brass loses its valuable physical and mechanical properties leading to structural failure. Brasses are technologically important materials used due to their excellent properties and have been highly studied, particularly in terms of dezincification [8], Localized or pitting corrosion [9,10] and stress corrosion cracking [9]. Different methods have been used to diagnose, evaluate, and control corrosion problems including distribution and plumbing system design considerations, water quality modifications, corrosion inhibitors, cathodic protection, and coatings and linings [10-12]. Many results suggest the passivation of brass may be attributed to the formation of a complex passive layer on brass consisting of mixtures of ZnO and Cu_xO_y, and with a composition strongly influenced by the anions of the solution [13-15].

One of the most important methods in corrosion protection is to use inhibitors [16-19], inhibitors should be of low toxicity and easily biodegradable in order to meet environmental protection requirements. Like CaCO_3 , these substances act as cathodic inhibitors and produce relatively thick films on the surface of the metal and have been used. Usually the films incorporate the corrosion products, as well as varying amounts of CaCO_3 . The successful formation of an inhibiting film and its continued good performance depend on a number of variables. These must be clearly understood and carefully controlled. Environmental restrictions imposed on heavy-metal based corrosion inhibitors, oriented scientific researches towards studying non-toxic and environmentally friendly corrosion inhibitors [20,21] and inhibitor used in drinking water was limited.

The objective of this study was to test an environmentally acceptable mineral inhibitor M1, family to the carbonated mineral rock, that would simultaneously inhibit corrosion by forming the continuous deposit and adherent on the metal surface. The inhibiting performance was evaluated by potentiodynamic curves and electrochemical impedance spectroscopy (EIS).

MATERIALS AND METHODS

Sample and preparation

The metal sample used in this study was brass (from National Drinking Water Office) used as tap water. The working electrode used having the chemical composition as wt (%) 56.24 Cu, 40.494 Zn, 2.345 Pb, 0.224 Fe, 0.2135 Sn, 0.114 Ni, 0.051 Al, 0.008 Mn, 0.003 As, and 0.0013 Si. This electrode was embedded in epoxy resin, leaving a geometrical surface area of 2.2 cm^2 exposed to the electrolyte. Prior to the measurements, the exposed surface was pre-treated by using decreased emery papers grade (400, 600, 1000, 1200 and 1500) and then rinsed by double distilled water.

Electrolyte

The experiments were carried out using artificial tap water (ATW) simulating the average composition of the drinking water. The mineral base composition was (110 mg/L $\text{CaCl}_2 \cdot 2\text{H}_2\text{O}$, 40 mg/L $\text{MgSO}_4 \cdot 7\text{H}_2\text{O}$, 60 mg/L $\text{MgCl}_2 \cdot 6\text{H}_2\text{O}$, 20 mg/L NaNO_3 , 470 mg/L Na_2CO_3 , 25 mg/L KNO_3) already used by other researcher [22]. Electrolyte pH was fixed at 7.6 ± 0.2 by titration 0.1 M HCl.

It is recognized that the high chloride, low hardness and low alkalinity waters are particularly prone dezincification of brass, which justifies the choice of this water. All experiments were performed at room temperature ($298 \pm 2\text{K}$).

Mineral compound characterization

Our study was focused to study the inhibition of mineral compound M1 as green inhibitor on brass in simulated drinking water which composition indicated type calcite (Figure 1).

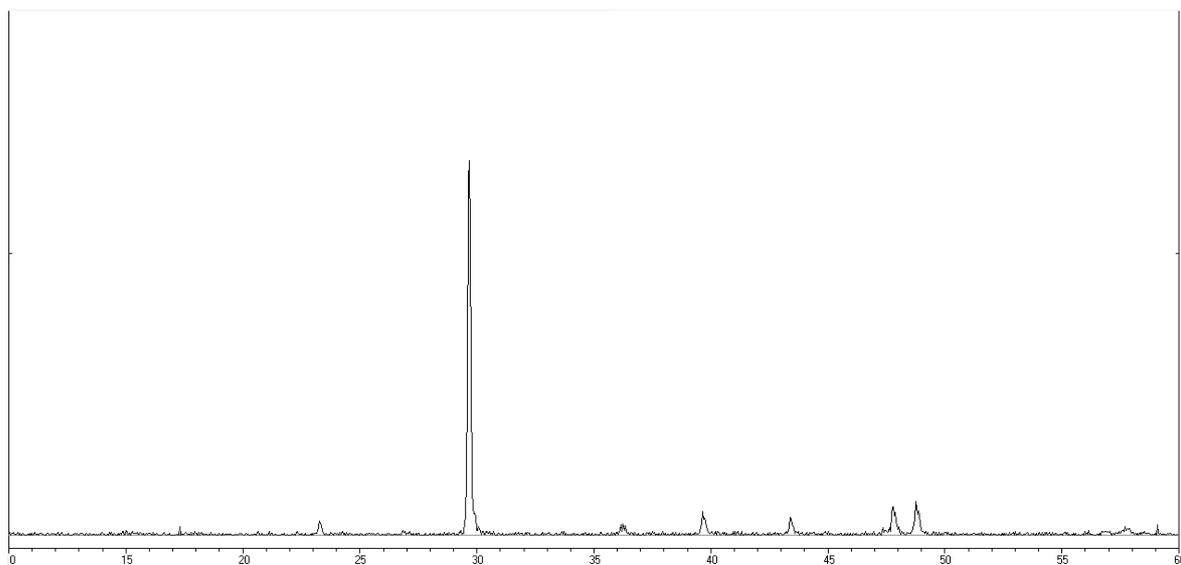


Figure 1: The XRD patterns of calcite

Electrochemical measurements

The electrochemical measurements were carried out using a potentiostat/galvanostat (Volta lab PGZ301). A three-electrode electrochemical cell and instrumentation employed are standard and have been reported before [23]. A saturated calomel electrode ((SCE) $E = 0.24$ V/SHE). A Luggin capillary minimized the Ohmic drop. A Pt wire was used as counter electrode. Brass electrodes were pre-reduced in the corresponding electrolyte at -1 V/SCE for 5 min to begin with a reproducible surface. Then, the electrodes were kept at the corrosion potential (E_{corr}) for 0.5 h. The passive layer was stable and the open circuit potential remained constant.

The potentiodynamic current-potential curves were recorded by changing the electrode potential automatically from -1000 to 1000 mV/SCE with scan rate of 1 mV s⁻¹. Electrochemical impedance spectroscopy (EIS) tests were performed at E_{corr} . The response of the electrochemical system to ac excitation with a frequency ranging from 100 KHz to 10 mHz and peak to peak amplitude of 10 mV was measured with data density of 10 points per decade. The impedance data were analyzed and fitted with the simulation Z-View 2.80, equivalent circuit software. All the measurements were carried out in air saturated solutions and at ambient temperature (298 ± 2 K). Each experiment was performed in a freshly prepared solution and with a newly ground electrode surface. The experiments were repeated to ensure reproducibility.

RESULTS AND DISCUSSION

Open circuit potential measurement

The values of open circuit potential of brass electrode at different concentration of M1 are present in Figure 2 at 298 K. The results illustrated that the open circuit potentials are shifted towards more positive direction for the blank and in presence of inhibitor at 20 ppm. Clearly, the initial OCP is -0.268 V in blank solution, and after increasing rapidly. About 400 s later, the value is almost constant at -0.120 V as time goes on, almost the same appearance was obtained in the presence of inhibitor at 20 ppm. When tests are conducted in the presence of inhibitor, decreased potential is observed to negative values all the more marked as the inhibitor concentration is important. The evolution of the free potential, in this case, indicates the formation of a protective layer film. The trial at 30 ppm and 40 ppm inhibitor has an intermediate evolution, namely stability (600 sec and 800 sec respectively) followed by a free ennoblement potential reflecting the formation of a protective film [24].

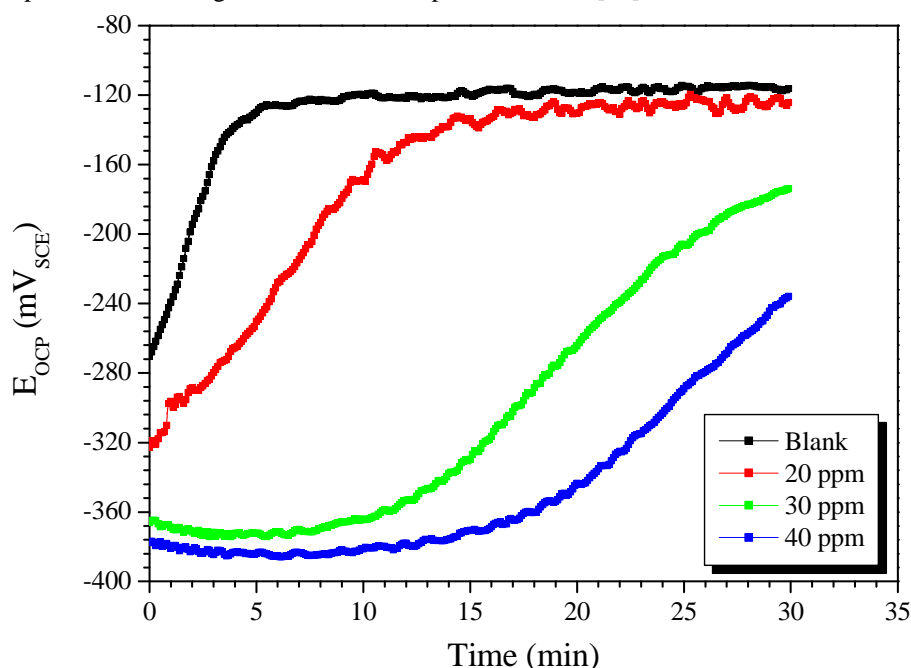


Figure 2: Open circuit potential as a function of exposure time in ATW solution with different concentrations of M1

Potentiodynamic polarization

Fig. 3 presents the potentiodynamic polarization curves of brass in ATW solutions without and with different concentrations of M1. It can be seen that the brass electrode displays a Tafel behavior of anodic region. As shown in the inset of Fig. 3, the Tafel line of the anodic polarization curve is extended to the electrode potential below the corrosion potential, and then a vertical line is made parallel to the Y-axis at the corrosion potential. The electrochemical parameters can be obtained from the point of intersection [25]. In addition, the Tafel slope can be obtained by the Tafel extrapolation method in accordance with the literature [26-29]. The electrochemical

parameters such as corrosion current density (I_{corr}), corrosion potential (E_{corr} vs. SCE), cathodic Tafel slope (β_c), anodic Tafel slope (β_a) and the inhibition efficiency ($\eta_{\text{pp}}\%$) are given in Table 1. The inhibition efficiency for each concentration of inhibitor is calculated using Eq. (1):

$$\eta_{\text{Tafel}} (\%) = \frac{i_{\text{corr}}^0 - i_{\text{corr}}}{i_{\text{corr}}^0} \times 100 \quad (1)$$

where i_{corr}^0 and i_{corr} are the corrosion current densities for brass electrode in the ATW solutions without and with M1, respectively.

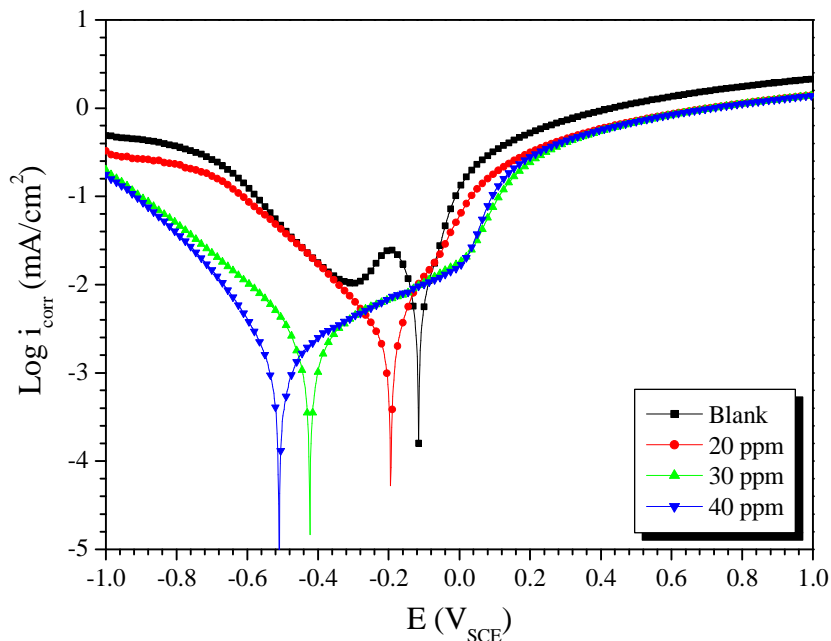


Figure 3: Potentiodynamic polarization curves for the brass electrode in artificial tap water (ATW) containing different concentrations of M1

It is known from Figure 3 that both the anodic and cathodic reactions of brass corrosion were suppressed in the presence of the studied inhibitor in artificial tap water (ATW) and the suppression effect increased with the increase in the concentrations of inhibitor. The optimum concentration used is 40 ppm. In the cathodic range, dissolved oxygen in the solution takes over the cathodic reaction of brass in ATW media as shown in the following Eq. (2)



In the anodic range, the dissolution of brass in drinking water is widely studied by several authors and is shown [13,15]:



Or



Then the dissolution of copper for the copper oxide formation Cu_2O and CuO :



Table 1: Potentiodynamic polarization parameters of brass in artificial tap water (ATW) solutions without and with the addition of M1 at different concentrations at 298 K

	Conc. (ppm)	$-E_{\text{corr}}$ (mV/SCE)	I_{corr} ($\mu\text{A}/\text{cm}^2$)	β_c (mV/dec)	β_a (mV/dec)	η_{Tafel} (%)
Blank	00	114.9	3.97	80.5	71.3	—
	20	192.9	1.92	194.5	99.7	51
M1	30	422.6	0.89	153.0	170.3	79
	40	443.6	0.67	129.4	139.2	84

The shift of E_{corr} values towards negative direction in the presence of M1 (Table 1 and figure 3), can be explained by the domination of cathodic reaction inhibition [30]. The change of potential in the negative direction can be attributed to the dissolution of native oxide and to the rapid formation of protective film on the brass surface, acting as barriers to the diffusion of oxygen molecules from the solution to the brass surface. However, it is clearly observed from the Fig. 3 that this inhibitor reduces both the anodic and cathodic current densities, indicating the inhibiting effect of the compound. The increase in β_a and β_c are related to the decrease in both the anodic and cathodic currents. This indicates that the M1 studied, inhibit the corrosion process of brass effectively and their ability as a corrosion inhibitor is enhanced as their concentration is increased.

It is widely acknowledged that an inhibitor can be classified as an anodic-or cathodic-type when the change in E_{corr} value is larger than 85 mV (SCE) [31,32]. If displacement in E_{corr} is < 85 mV, the inhibitor can be seen as mixed type. In comparison with the brass in the blank, the E_{corr} values move more in the negative direction, and the displacements are more than 85 mV (SCE). Therefore, it confirms that M1 is cathodic-type corrosion inhibitor and hinders the cathodic reaction by adsorbing on the brass surface.

Electrochemical Impedance Spectroscopic measurements

To further study interfacial changes at the brass surface with and without inhibitor addition, electrochemical impedance measurements have been carried out. Fig. 4 shows the obtained Nyquist plots of brass in artificial tap water (ATW) solutions containing different inhibitor concentrations ranged from 20 ppm to 40 ppm after 0.5 h of immersion. The semi-circular depression in the Nyquist diagram was attributed to the heterogeneity of the surface, the surface roughness and the existence of two different processes having practically the same relaxation time. The increase in the diameter of the arc indicated that there is the improvement of a more capacitive surface film, promoting the formation of the protective layer.

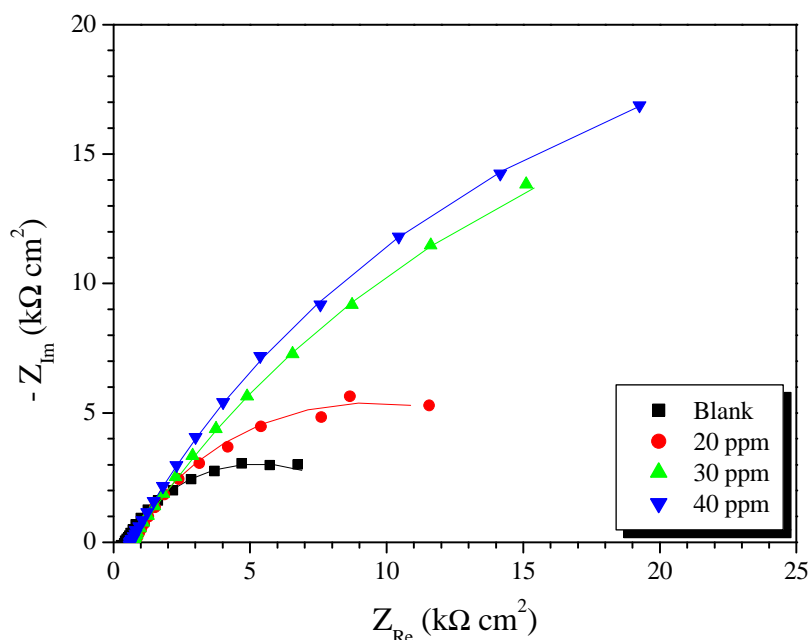


Figure 4: Nyquist plots of brass specimens in artificial tap water (ATW) solution containing various concentrations of inhibitor. Symbols: Experimental data and Red continuous lines: Fitting data



Figure 5: Proposed equivalent circuits for impedance analysis and interpretation of brass-ATW solution system. Equivalent circuit for having (a) one semi circle (b) two semicircles in impedance spectra

It is clear observed from these figures that Nyquist plots yield only one slightly depressed semi-circle in the uninhibited solution and low concentration inhibited solutions. This indicates that the brass corrosion in blank solution is mainly controlled by a charge transfer process [33]. Electrical equivalent circuits used for modeling of this metal/solution interface have one semi-circle; represented in Fig. 5a. One semi-circle in Nyquist diagrams associated with the relaxation process of the double layer dominated and obtained R_{ct} was a sum of the electric double layer and adsorption layer effects because they could not be split up [34]. R_{ct} is the charge transfer resistance whose value is a measure of electron transfer across the surface, R_d is the diffuse layer resistance, and CPE_{dl} is the constant phase element of the double layer. Here, the sum of R_{ct} and R_d resistances are equal to R_p which is the polarization resistance ($R_p = R_{ct} + R_d$). The second loop that can be observed in the Nyquist diagrams of inhibitor free solutions was related with the oxide layer on brass formed in ATW-solution. In these cases there were no inhibitor molecules in the solution, so the film resistance R_f should not take part in the polarization resistance expression. The total resistance may be stated as $R_p = R_{ct} + R_d + R_{ox}$ and CPE_f was related to the oxide film of brass. The Nyquist plots contain depressed semicircles with the center under the real axis; such behavior is characteristic of solid electrodes and often referred to as frequency dispersion. This type of Nyquist diagram was characterized by distributed capacitance. It is necessary to use a constant phase element, CPE, instead of double layer capacity to account for the non-ideal behavior [34]. The CPE element is used to explain the depression of the capacitance semi-circle, which corresponds to surface heterogeneity resulting from surface roughness, impurities, dislocations, grain boundaries, adsorption of inhibitors, and the like [35]. The deviation of Nyquist from the ideal behavior of the metal-solution interface could be explained by the stacking of the big-bodied molecule to the OHP (Outer Helmholtz Plane) layer.

The impedance of this element is frequency dependent and can be mathematically expressed as Eq. (8):

$$Z_{CPE} = \frac{1}{Y_0 (j\omega)^n} \quad (8)$$

where Y_0 is the CPE constant, n is the CPE exponent. j is the square root of -1, and ω is the angular frequency. Depending on the value of n , CPE can represent a resistance. n is a measure of non-ideality of the capacitor and has a value ranging from -1 to 1 [36].

The equivalent circuit related to the electrochemical process which has two loops in the Nyquist diagram is given in Fig. 5b. Here, the polarization resistance (R_p) is equal to the sum of the charge transfer resistance (R_{ct}), diffuse layer resistance (R_d), R_{ox} the oxide film resistance that formed on brass surface and film resistance (R_f) values ($R_p = R_{ct} + R_d + R_{ox} + R_f$) and CPE_f was the capacitance of both oxide and complex film layer.

As seen from Fig. 4, the R_p values increased with the M1 concentration, which can be attributed to the formation of a protective over-layer at the metal surface, which becomes a barrier for the mass and the charge transfers.

The electrochemical and fitting parameters for solutions with and without M1 are listed in Table 2. According to Table 2, decreases in the CPE values and increases in the R_p values were related to the adsorption of M1 molecules onto the metal surface and the formation of an insulated adsorption layer.

Table 2: Impedance parameters for brass corrosion in ATW-solution at different concentration of M1

	Conc. (ppm)	R_s ($\Omega \text{ cm}^2$)	CPE_{dl}		$R_{ct}+R_d$ ($\Omega \text{ cm}^2$)	CPE_f		R_f+R_{ox} ($\Omega \text{ cm}^2$)	R_p ($\Omega \text{ cm}^2$)	η_{EIS} (%)
			$Y_0 \times 10^4$ ($S^n \Omega \text{ cm}^{-2}$)	n_{dl}		$Y_0 \times 10^4$ ($S^n \Omega \text{ cm}^{-2}$)	n_f			
Blank	00	201.8	1.9926	0.71	4761	—	—	—	4761	—
	20	321.7	1.0762	0.66	10234	0.6570	0.88	229	10463	57.2
M1	30	281.4	0.8999	0.70	18456	0.3349	0.65	10567	29023	83.6
	40	312.1	0.2877	0.71	32421	0.1525	0.67	10950	43371	89.0

The inhibition efficiencies (η_{EIS}) were calculated by using the difference between the real impedance values at lower and higher frequencies according to the following equation.

$$\eta_{EIS} (\%) = \frac{R_{p(inh)} - R_p}{R_{p(inh)}} \times 100$$

(9)

where $R_{p(inh)}$ and R_p are polarization resistance values with and without M1, respectively.

CONCLUSION

In this study, inhibitive behaviors of mineral compound M1 was used as green inhibitor for brass in artificial tap water (ATW) have been investigated and following outcomes have been obtained:

- ✓ Inhibition performance values increase with increasing inhibitor concentration M1 and have shown an inhibition corrosion maximum of 89 % at 40 ppm.
- ✓ According to the results, the mineral inhibitor M1 has a significant effect on the shift potential values in negative direction. Therefore, it is concluded that the mineral compound M1 acts as the cathodic- type inhibitor.
- ✓ Impedance diagram shows that the size of the loop impedance increases with presence inhibitor, two constants time were detected, confirming the formation of a protective layer which results the continuous deposit and adherent on the metal.
- ✓ The measures EIS and polarization curves are in good agreement.

REFERENCES

- [1] A. El Warraky, H.A. El Shayeb, E.M. Sherif, *Anti-Corros. Methods Mater.* **2004**, 51, 52.
- [2] E.M. Sherif, R.M. Erasmus, J.D. Comins, *J. Colloid Interface Sci.* **2007**, 309, 470.
- [3] G. Quartarone, G. Moretti, T. Bellomi, *Corrosion*, **1998**, 54, 606.
- [4] Q. Qu, S. Jiang, W. Bai, L. Li, *Electrochim. Acta*, **2007**, 52, 6811.
- [5] M.A. Quraishi, R. Sardar, *Corrosion*, **2002**, 58, 748.
- [6] S. Zor, P. Doğan, B. Yazici, *Corros. Sci.* **2005**, 47, 2700.
- [7] S.T. Selvi, V. Raman, N. Rajendran, *J. Appl. Electrochem.* **2003**, 33, 1175.
- [8] K. Habib, *Corros. Sci.* **1998**, 40, 1435.
- [9] X.S. Du, Y.J. Su, J.X. Li, L.J. Qiao, W.Y. Chu, *Corros. Sci.* **2012**, 60, 69.
- [10] E. Sarver, M. Edwards, *Corros. Sci.* **2011**, 53, 1813.
- [11] M. R. Schock, *Corrosion*, **1996**, 96, 24.
- [12] M. Salasi, T. Shahrabi, E. Roayaei, M. Aliofkhaezraei, *Mater. Chem. Phys.* **2007**, 104, 183
- [13] L. Yohai, M. Vázquez, M. B. Valcarce, *Corros. Sci.* **2011**, 53, 1130.
- [14] P. Qiu and C. Leygraf, *Appl. Surf. Sci.* **2011**, 258, 1235.
- [15] T. K. Mikić, I. Milošev, B. Pihlar, *J. Appl. Electrochem.* **2005**, 35, 975.
- [16] Y. Tang, W. Yang, X. Yin, Y. Liu, P. Yin, J. Wang, *Desalination*, **2008**, 228, 55.
- [17] T. Y. Soror, *Open Corros. J.* **2009**, 2, 45.
- [18] N. S. Grigg, *Secondary impacts of corrosion control on distribution system and treatment plant equipment*, Water Research Foundation, **2010**.
- [19] A. Angamuthu, C. Thangavelu, S. Rajendran, T. Asokan, *Zašt. Mater.* **2012**, 53, 9.
- [20] D.-J. Choi, S.-J. You, J.-G. Kim, *Mater. Sci. Eng. A* **2002**, 335, 228.
- [21] M. Nihorimbere, Y. Kerroum, A. Guenbour, M. Kacimi, A. Bellaouchou, R. Tourir, A. Zarrouk, *J. Mater. Environ. Sci.* 7 (11), **2016**, 4121.
- [22] M. B. Valcarce, S. R. De Sanchez, M. Vazquez, *Electrochimica. Acta*, **2006**, 51, 3736.
- [23] M.B. Valcarce, M. Vázquez, *Corros. Sci.* **2010**, 2, 1413.
- [24] W. A. Badawy, F. M. Al-Kharafi, *Corrosion*, **1999**, 55, 268.
- [25] S. Hong, W. Chen, H.Q. Luo, N.B. Li, *Corros. Sci.* **2012**, 57, 270.
- [26] F. Mansfeld, *Corros. Sci.* **2005**, 47, 3178.
- [27] R.F. Sandenbergh, E. Van der Lingen, *Corros. Sci.* **2005**, 47, 3300.
- [28] Harvey J. Flitt, D. Paul Schweinsberg, *Corros. Sci.* **2010**, 52, 1905.
- [29] E. McCafferty, *Corros. Sci.* **2005**, 47, 3202.
- [30] C.I.S. Santos, M.H. Mendonca, I.T.E. Fonseca, *J. Appl. Electrochem.* **2006**, 36, 1353
- [31] A.Y. Musa, A.A.H. Kadhum, A.B. Mohamad, M.S. Takriff, A.R. Daud, S.K. Kamarudin, *Corros. Sci.* **2010**, 52, 526.
- [32] W. Li, Q. He, S. Zhang, C. Pei, B. Hou, *J. Appl. Electrochem.* **2008**, 38, 289.
- [33] R. Solmaz, G. Kardas, M. Culha, *Electrochim. Acta*, **2008**, 53, 5941.
- [34] H. Keleş, *Mater. Chem. Phys.* **2011**, 130, 1317.
- [35] S.A. Kumar, M.A. Quraishi, *Mater. Chem. Phys.* **2010**, 123, 666
- [36] N.A. Negm, M.F. Zaki, M.M. Said, S.M. Morsy, *Corros. Sci.* **2011**, 53, 4233.